

JOURNAL OF ENVIRONMENTAL GEOGRAPHY  
*Journal of Environmental Geography* 9 (1–2), 23–30.  
 DOI: 10.1515/jengeo-2016-0004  
 ISSN: 2060-467X



## SATELLITE BASED ANALYSIS OF SURFACE URBAN HEAT ISLAND INTENSITY

Orsolya Gémes, Zalán Tobak\*, Boudewijn van Leeuwen

Department of Physical Geography and Geoinformatics, University of Szeged, H-6722, Egyetem u. 2-6, Hungary

\*Corresponding author, e-mail: [tobak@geo.u-szeged.hu](mailto:tobak@geo.u-szeged.hu)

Research article, received 1 May 2016, accepted 1 June 2016

### Abstract

The most obvious characteristics of urban climate are higher air and surface temperatures compared to rural areas and large spatial variation of meteorological parameters within the city. This research examines the long term and seasonal development of urban surface temperature using satellite data during a period of 30 years and within a year. The medium resolution Landsat data were (pre)processed using open source tools. Besides the analysis of the long term and seasonal changes in land surface temperature within a city, also its relationship with changes in the vegetation cover was investigated. Different urban districts and local climate zones showed varying strength of correlation. The temperature difference between urban surfaces and surroundings is defined as surface urban heat island (SUHI). Its development shows remarkable seasonal and spatial anomalies. The satellite images can be applied to visualize and analyze the SUHI, although they were not collected at midday and early afternoon, when the phenomenon is normally at its maximum. The applied methodology is based on free data and software and requires minimal user interaction. Using the results new urban developments (new built up and green areas) can be planned, that help mitigate the negative effects of urban climate.

**Keywords:** urban LST, urban heat island, Landsat

### INTRODUCTION

Although, fifty three percent of the world's population lives in cities, according to the estimations only 3% of the continents is urban area (World Bank, 2014). This relatively small area is intensively used and continuously affects its inhabitants by providing them a dynamically changing residential environment.

The climate of the horizontally and vertically diverse urban surface is influenced by several factors on macro and meso (e.g. climate, elevation, relief), as well as local level. Local modifying factors, not active in non urban areas are (1) the generally higher specific heat and low albedo of anthropogenic surfaces, (2) modified water regime resulting in lower air humidity, (3) the special surface geometry modifying the flow conditions, (4) the periodical heat surplus (due to heating, traffic or industry) and (5) the increased atmospheric aerosol concentration (Unger, 1996). On meso level the impact of urban surfaces can be detected up to 9-11km (urban boundary layer – UBL), and local micro-level processes have effects up to the average roof-top level (urban canopy layer – UCL) (Oke, 1976).

The total energy balance of urban areas is similar to the rural areas, however, there are differences in the ratio of shortwave and longwave radiation. Due to the high aerosol concentration the incoming direct, diffuse and atmospherically reflected shortwave radiation is low, and the shortwave radiation reflected from the surface is also low due to the low albedo. The

warmer surfaces result in higher longwave radiation, furthermore air pollution increases the reflected and diffuse longwave radiation (Unger, 2010a).

Urban heat islands (UHI) are typical microclimatic phenomena in urban areas. The air temperature of urban areas is significantly higher at night compared to the rural areas (Landsberg, 1981). The phenomenon has a horizontal as well as a vertical character. According to the typical UHI thermal profile a steep temperature gradient occurs at the rural/urban boundaries (cliff), and thereafter the temperature increases along steady horizontal gradient (plateau) and the highest temperature is at the urban centre (peak). Vertically the positive temperature anomaly can be detected reach up to 200-300 meters (Unger, 2010a). In general, a 0.5-1°C positive anomaly can be identified in urban areas compared to rural areas depending on the density and extent of built-up areas. Local urban climate is a phenomenon formed by several complex processes (Probáld, 1974).

Several publications appeared that use aerial and satellite remote sensing data to study the changing urban environment due to the dynamically increasing population. Considering the current study a significant advancement was the assessment of Roth et al. (1989), who used infrared (NIR) band of NOAA AVHRR satellite to monitor surface temperature. According to their experiences the pattern of heat release had a stronger correlation with the land cover during the day compared to the night. It is contradictory to the results calculated from measured air tem-

perature values at 2-3m height above the surface. Nichol (2005) compared ASTER night-time thermal infrared data with Landsat 7 (ETM+) daytime data to study the relationship between surface temperature and urban morphology during a daily temperature cycle. The research found the meso scale processes more important in the UBL at night, while during the day they were significant rather in the UCL. Purnhauser (2001) investigated the urban climate of Szeged in different seasons and used the sky view factor (SVF) defined by Oke (1988). It was found that in open, green areas the longwave radiation is significant; in narrow streets with high buildings an ‘urban canyon effect’ was observed, because the longwave radiation was trapped decreasing the loss of radiation to the atmosphere. Soósné (2009) assessed the urban climate of Hungarian and Central European cities using surface temperature, land cover and vegetation indices data from the MODIS sensor, and ASTER surface temperature data. She evaluated the spatial pattern of UHI in all 4 seasons and in 4 periods during a day (dawn – morning – afternoon – evening). Gábor and Jombach (2009) used Landsat TM data to investigate the relationship between 14 different land use class and the surface temperature. The spatial pattern and intensity of UHI in Szeged were assessed and evaluated by Unger et al. (2010b) using measured air temperature field measurements and surface temperature datasets acquired by an airborne remote sensing system.

## STUDY AREA

Urban climate is highly dependent on population density. In Hungary 70% of the population lives in urban areas (in 346 towns and cities in total) (KSH, 2015). Szeged is the third most populous city in Hungary (with 163000 inhabitants). The number of inhabitants was increasing until the 1990s, and afterwards a decreasing tendency has been observed. The reasons behind the changes are the countrywide characteristic natural decrease of the population, furthermore, the migration of the people to the neighbouring villages. A migration surplus can be observed in Szeged since 2007 (KSH, 2015).

The macroclimate of an area also influences the urban climate. Hungary, and therefore Szeged being located on the South Hungarian Great Plain (Fig. 1), belong to the temperate zone; Cf type of Köppen’s climate zones (warm continental climate and with significant precipitation in all seasons). Péczely (1979) categorised Szeged into the warm-dry climate zone based on its water and heat balance. The annual mean temperature, the mean summer temperature and the mean annual precipitation are 10.6°C, 20.3°C, and 489mm, respectively. The average total hours of sunshine at Szeged is 250-280 in summer months and 50-80 in winter months (OMSZ, 2016).

The city structure is characterised by avenues and boulevards built during the reconstructions after the great flood in 1879. The river Tisza divides the city in two parts: Southeast from the river, the area is mostly characterised by larger urban green areas and, family

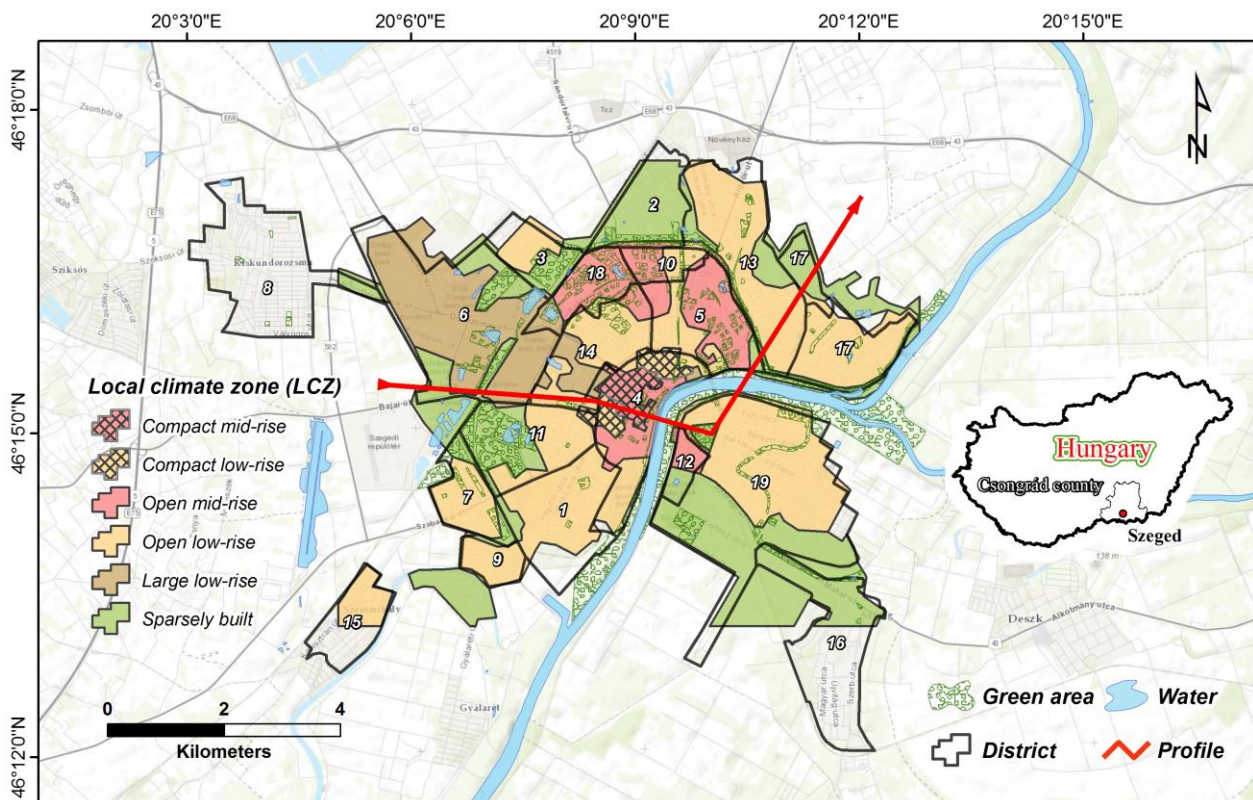


Fig. 1 Study area (1 Alsóváros, 2 Baktó, 3 Béke-telep, 4 Belváros, 5 Felsőváros, 6 Iparváros, 7 Kecskes, 8 Kiskundorozsma, 9 Klebsbergtelep, 10 Makkosháza-Fodorkert, 11 Móraváros, 12 Odessza, 13 Petőfi-telep, 14 Rókus, 15 Szentmihály, 16 Szöreg, 17 Tápé, 18 Újrókus, 19 Újszeged)

houses with gardens. North of the river the city centre, housing estates and industrial areas can also be found (Fig. 1).

For the uniform description of the local climate features a Local Climate Zone (LCZ) classification was developed. The categories can be well applied on plains, where the influence of the relief on the climate is less strong than in areas with large height differences (Stewart and Oke, 2012). The categories were defined based on the land cover, resulting in 10 urban and 6 rural categories. The first 3 urban categories are characterised by mainly built-up areas, green areas are represented only by a few trees. In the case of the following 3 categories the ratio of green cover is increasing, and the rest of the categories have open green areas and low built-up density. Lelovics et al. (2014) mapped the local climate zones in Szeged (Fig. 1) using a building database, aerial photos, topographical maps, RapidEye satellite images, an infrastructure database, SVF values, building height and roughness data, albedo values of the different surfaces, NDVI images and CLC land cover data. The following categories were identified in their work in the city of Szeged: (2) compact mid-rise, (3) compact low-rise, (5) open mid-rise, (6) open low-rise, (8) large low-rise and (9) sparsely built.

## DATA AND METHODS

Landsat 4, 5 TM, Landsat 7 ETM+, and Landsat 8 OLI/TIRS data from the period between 1984 and 2016 were applied in this research (Table 1). For the long-term assessment, images from the same period in July, with a 10 year interval were evaluated describing summer conditions. Interannual changes were assessed using one image for each season between 2015 and 2016.

The raw (DN) pixel values were processed using the Semi Automatic Classification Plugin (SCP) of the open source QGIS software (SCP) along two parallel workflows (Fig. 2). On one hand the data of the thermal band was processed, on the other hand a supervised classification was carried out on the visible and infrared bands. Emissivity values assigned to each class were applied during the land surface temperature (LST) calculations.

The data sets used for the analyses needed to be preprocessed to land surface temperature. Each data set was preprocessed using a data specific workflow that does not use any ancillary data. During the first step, the raw digital numbers (DN) of the TM, ETM+ and OLI sensors were converted to at-satellite or top-of-atmosphere (ToA) spectral radiances ( $L_\lambda$  in  $\text{Wm}^{-2}\text{sr}^{-1}\mu\text{m}^{-1}$ ) using:

$$L_\lambda = M_L * Q_{cal} + A_L \quad (1)$$

where  $M_L$  and  $A_L$  are respectively the band-specific multiplicative rescaling factor and the additive rescaling factor, which are both available from the metadata.  $Q_{cal}$  is the quantized and calibrated standard product pixel values (DN). In the next step, the ToA radiances of the visible to SWIR bands were converted to unitless ToA reflectances  $\rho_p$  by:

$$\rho_p = \pi * L_\lambda * d^2 * (ESUN_\lambda * \cos(\theta_s))^{-1} \quad (2)$$

where  $d$  is the Earth-Sun distance in astronomical units at the acquisition time,  $ESUN_\lambda$  is the band specific mean solar exo-atmospheric irradiances, and  $\theta_s$  is the solar zenith angle in degrees, which is equal to  $\theta_s = 90^\circ - \theta_e$  where  $\theta_e$  is the sun elevation as given in the metadata. To derive the surface reflectance, it was required to apply some sort of atmospheric correction. In this research, no detailed data was available about the state of the atmosphere at the time of the data acquisition, therefore the Dark Object Subtraction (DOS) method (Moran et al., 1992) was applied to the data sets assuming that within an image some pixels are in complete shadow and their radiances received at the satellite are due to atmospheric scattering (Chavez, 1996). The surface reflectance is then:

$$\rho_s = [\pi * (L_\lambda - L_p) * d^2] * (ESUN_\lambda * \cos(\theta_s))^{-1} \quad (3)$$

where  $L_p$  is the path radiance (Sobrino et al., 2004):

$$L_p = M_L * DN_{min} + A_L - 0.01 * ESUN_\lambda * \cos(\theta_s) * (\pi * d^2)^{-1} \quad (4)$$

The surface reflectance values were used to classify the data with the spectral angle mapping algorithm (Kruse et al., 1993) into 4 land cover classes (water, vegetation, bare soil, built up) and to calculate NDVI values. The thermal bands were converted to at-satellite brightness temperature by:

Table 1 Satellite images (A: long-term / B: seasonal assessment) and meteorological data (OMSZ, OGIMET) used in the assessment

| Sensor             | Acquisition date/time      | Pixel size (VNIR/TIR) [m] | Daily mean temperature [°C] | Daily maximum temperature [°C] | VIS (km) |
|--------------------|----------------------------|---------------------------|-----------------------------|--------------------------------|----------|
| Landsat 4 TM       | 31-Jul-1984 <sup>A</sup>   | 30/120                    | 22.8                        | 30.3                           | n.a.     |
| Landsat 5 TM       | 27-Jul-1994 <sup>A</sup>   |                           | 25.0                        | 34.0                           | n.a.     |
| Landsat 7 ETM+     | 22-Jul-2004 <sup>A</sup>   | 30/60                     | 26.4                        | 34.6                           | 28       |
| Landsat 8 OLI/TIRS | 18-May-2015 <sup>B</sup>   | 30/100                    | 16.9                        | 24.1                           | 50       |
|                    | 21-Jul-2015 <sup>A,B</sup> |                           | 25.3                        | 32.4                           | 70       |
|                    | 23-Sep-2015 <sup>B</sup>   |                           | 17.5                        | 23.1                           | 15       |
|                    | 22-Feb-2016 <sup>B</sup>   |                           | 7.0                         | 10.7                           | 50       |



$$T_{b\lambda} = K_2 * \left( \ln \left( \frac{K_1}{L\lambda} + 1 \right) \right)^{-1} \quad (5)$$

not possible to apply the split window algorithm on Landsat 8 data (USGS Landsat 8, 2016), empirical emissivity values  $e$  (Weng et al., 2004; Mallick et al., 2012) for the earlier derived land cover classes were used with the following formula to convert the brightness temperatures to surface temperature:

$$T_{s\lambda} = T_{b\lambda} / [ 1 + (\lambda * T_{b\lambda} / p) \ln(e) ] \quad (6)$$

where  $\lambda$  is the wavelength of emitted radiance, and

$$p = h * c / s (1.438 * 10^{-2} \text{ m K}) \quad (7)$$

with  $h$  is Planck's constant,  $s$  is Boltzmann constant, and  $c$  is the velocity of light.

The surface urban heat island (SUHI) intensity can be defined as the difference between the temperature of urban and rural areas at ground level. Szeged meteorological station and its 750 m wide buffer zone was used as reference region in this study. This area was also used

as reference for previous air temperature measurements of an urban climate research by Unger (2010a). It accurately represents the main land cover types around the city (arable land, meadow-pasture, and forest).

The spatial pattern of the SUHI intensity was analysed for the whole city and along a profile. The initial point of this line was the centre point of the reference area, the Szeged meteorological station (Fig. 1). During the allocation of the profile it was important to cross Iparváros (an industrial area), areas of different built-up ratio and vegetation cover

In this research the following main questions were addressed:

- 1) How the pattern of LST changed during the investigated 30 years in Szeged? What is the relationship between the ratio of built-up areas/vegetation cover and the calculated LST values?
- 2) How the intensity of surface urban heat island (SUHI) changed compared to the reference rural zone in the investigated period?
- 3) What is the interannual pattern of LST in the predefined local climate zones?
- 4) What are the characteristic seasonal features of the spatial pattern of SUHI?

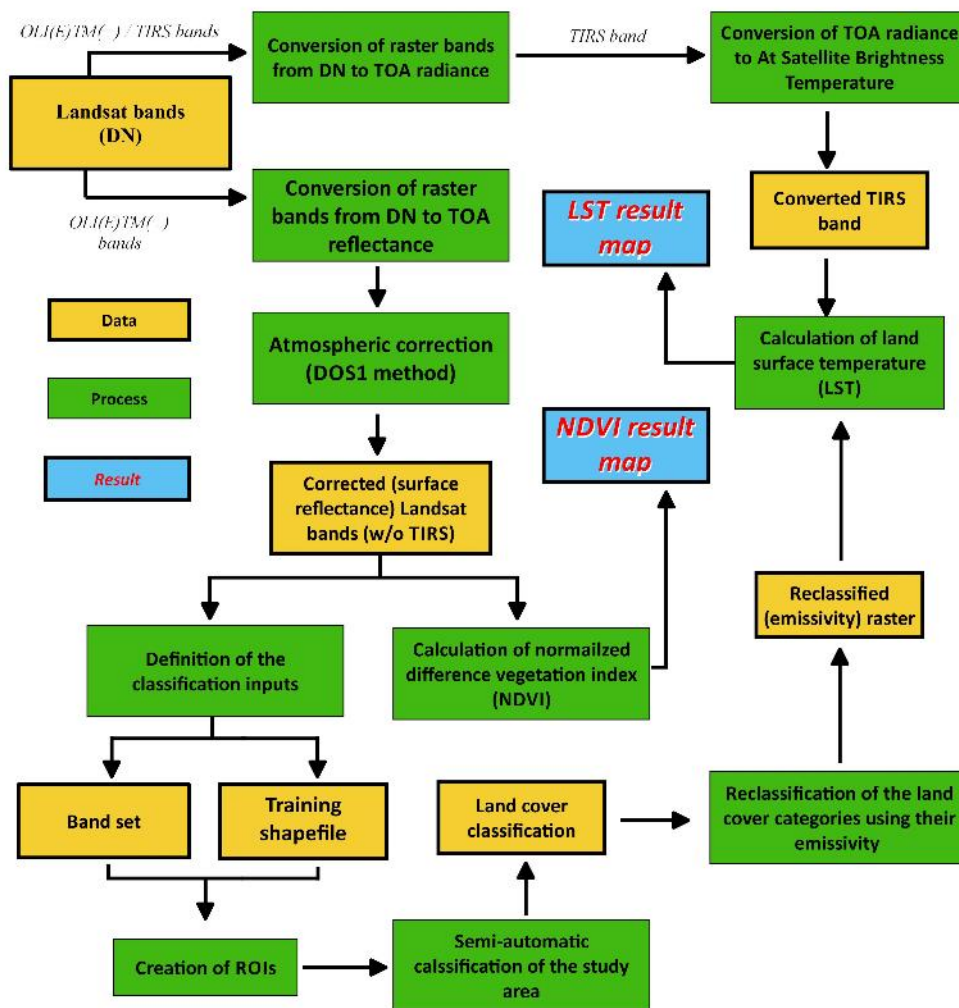


Fig. 2 Workflow of LST calculation in QGIS using Semi Automatic Classification plugin

## RESULTS

Daytime surface temperature images with 30 m spatial resolution were prepared for nearly the same summer day in 1984, 1994, 2004 and 2015, and for one day in each season at same time intervals between spring 2015 and winter 2016 for the city of Szeged. For the same dates NDVI values were calculated in 30 m spatial resolution using the red and infrared bands in the data sets.

During image selection important criteria were the lack of cloud cover, since it reflects characteristic weather conditions in the given seasons and the absence of precipitation. The appropriate conditions were checked and confirmed by meteorological datasets (Table 1).

### *LST and NDVI between 1984 and 2015 in the investigated urban districts*

The most significant changes of built up areas were observed between 1984 and 2004 (Fig. 3). In the investigated 30-years-long period the highest difference between the mean LST values was observed in the case of Petőfi-telep exceeding even 7°C. LST decrease was observed in none of the investigated districts (Table 2).

Table 2 Changes of LST and NDVI in city districts in the investigated 30 years

|    | District             | $\Delta$ LST | $\Delta$ NDVI |
|----|----------------------|--------------|---------------|
| 1  | Alsóváros            | 5.76         | 0.09          |
| 2  | Baktó                | 5.27         | 0.12          |
| 3  | Béke-telep           | 6.30         | 0.06          |
| 4  | Belváros             | 5.48         | 0.15          |
| 5  | Felsovaros           | 5.33         | 0.19          |
| 6  | Iparváros            | 6.55         | 0.04          |
| 7  | Kecskes              | 4.78         | 0.09          |
| 8  | Kiskundorozsma       | 5.69         | 0.06          |
| 9  | Klebensbergtelep     | 6.20         | 0.08          |
| 10 | Makkosháza-Fodorkert | 5.84         | 0.17          |
| 11 | Móráváros            | 5.83         | 0.09          |
| 12 | Odessza              | 3.30         | 0.21          |
| 13 | Petőfi-telep         | 7.08         | 0.04          |
| 14 | Rókus                | 6.11         | 0.10          |
| 15 | Szentmihály          | 5.38         | 0.06          |
| 16 | Szőreg               | 6.10         | 0.03          |
| 17 | Tápé                 | 6.51         | 0.03          |
| 18 | Újrókus              | 6.44         | 0.10          |
| 19 | Újszeged             | 6.24         | 0.06          |

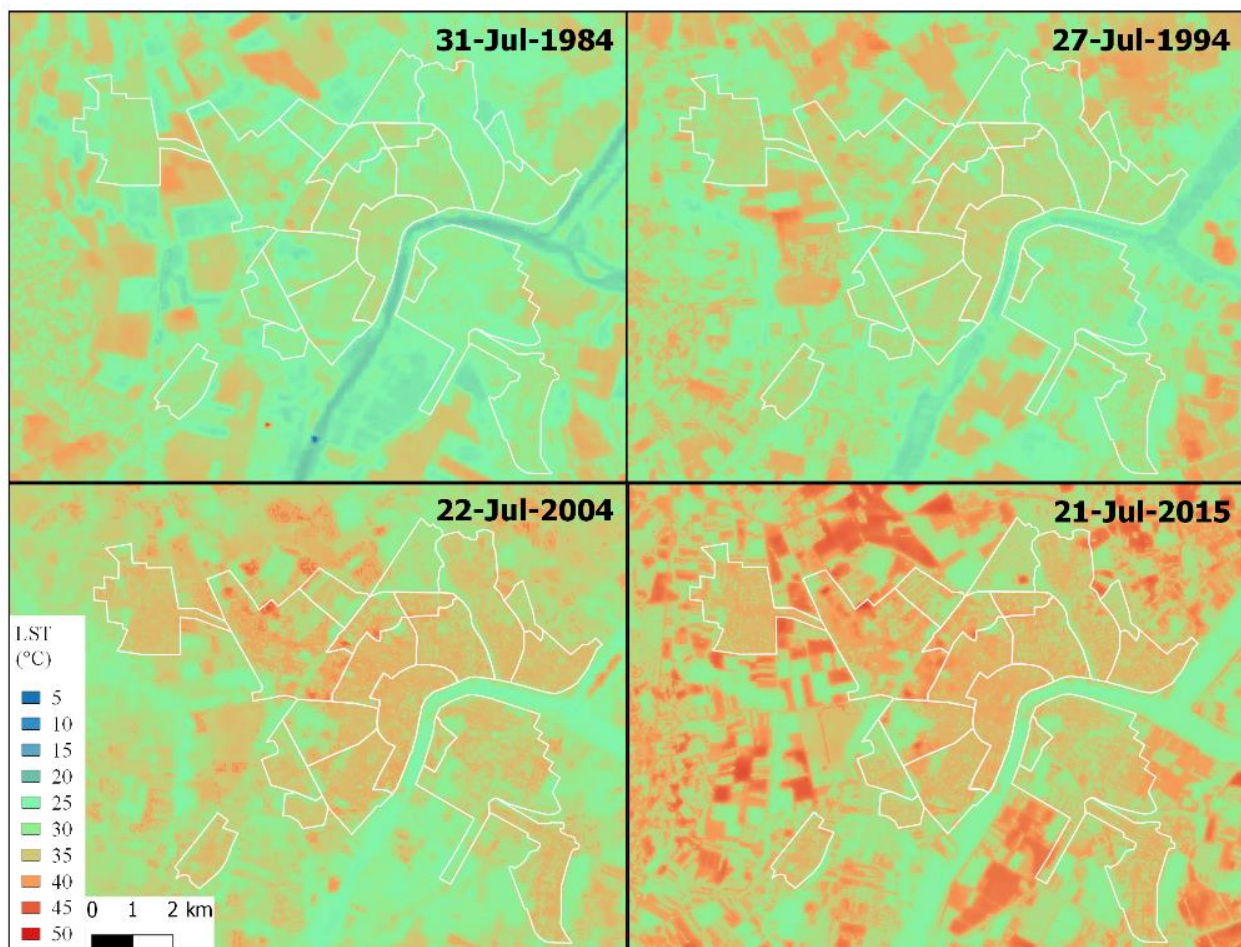


Fig. 3 Changes of LST between 1984 and 2015



The observed slight changes in NDVI values were in concordance with the significant increase of the temperature (e.g. in the case of Szőreg, Petőfi-telep, Iparváros). In those districts where a larger increase in vegetation cover occurred, only lower LST values were detected (e.g. Odessza). The most spectacular changes happened at such areas where vegetation was replaced by built-up areas (e.g. shopping malls, industrial areas). A relatively strong correlation ( $R=-0.69$ ) between the vegetation indices and the changes in the surface temperature values can be identified. However, vegetation seems to be a major determining factor of LST changes, the surface material (albedo) and its geometry, furthermore the actual weather conditions also significantly impact the LST changes.

*Spatial pattern of daily SUHI intensity*

Based on LST values, the phenomenon of surface urban heat island was the most observable at midday and early afternoon, however urban heat islands based on the measured air temperature differences are the most pronounced at night. The applied Landsat images were captured between 9.30 and 10.30, thus they were not expected to show the highest differences (namely the maximum of SUHI intensity) compared to the rural areas. Apart from this, the temperature of the built-up urban areas significantly exceeded the mean temperature of the rural areas (Fig. 4). The highest positive intensity was observed at the industrial areas in all cases, and the rate exceeded 10°C even in this morning period. The minimum values

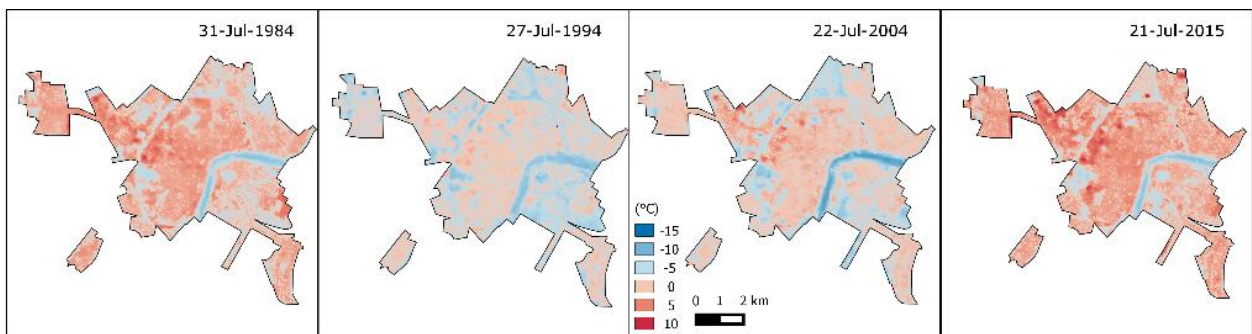


Fig. 4 UHI intensity compared to the rural areas

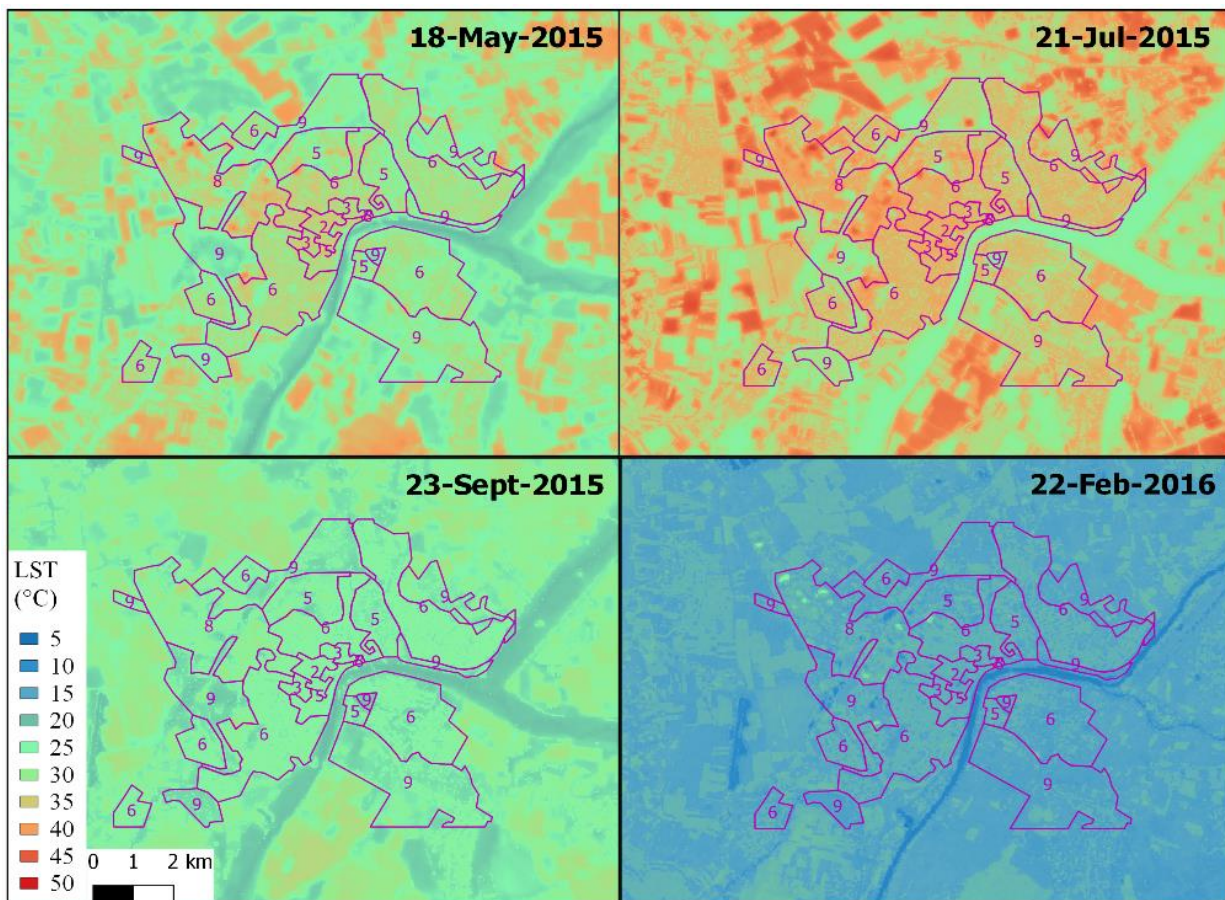


Fig. 5 Seasonal patterns of LST (2 Compact midrise, 3 Compact low-rise, 5 Open midrise, 6 Open low-rise, 8 Large low-rise, 9 Sparsely built)

were detected in the case of larger urban green areas (e.g. parks, floodplain) and the water surface of the River Tisza.

The highest mean positive SUHI intensity was detected in the densely populated city centre and Rókus districts on two out of the 4 investigated dates. The smallest mean difference was identified in a district of the outskirts area, in Baktó and once in the suburban Új-Szeged district. The least variation in temperatures was found in the city centre, while the industrial areas showed the highest standard deviation. The average difference between the surface temperature in urban and rural areas was + 1.5°C in 2015.

#### Seasonal changes of urban LST in the local climate zones

According to the seasonal comparison (Fig. 5) the lowest LST values were detected in the sparsely built LCZ category in spring, summer and autumn (Table 3), where the land cover has characteristically a lower ratio of built-up areas, but more gardens and sporadic tree cover. In winter the lowest LST values were detected in the open low-rise LCZ category, which consists of mostly open areas characterized by low buildings. The differences in minimum values in winter are due to the smaller influence of vegetation. The maximum temperature values occurred in the large low-rise category in all seasons, which are mostly built up areas without vegetation. These are typically the territories of large shopping malls and their parking lots.

A significant negative correlation ( $-0.68 < R < -0.87$ ) between the NDVI and LST values in the vegetation period was observed in the investigated districts. The lowest correlation was detected in the city centre, due to the lower vegetation cover (Table 4).

#### Daytime SUHI intensity along a profile in the city

The profile represents the influence of the different land cover types on surface temperature. The line intersects the River Tisza at two locations and has a 2800 m long suburban section as well. This section shows significant deviations in the different seasons (Fig. 6). The reason for this is the seasonal change of vegetation on arable lands. After the line reaches the border of the urban zone (at 2850 m), there is a significant change of the forest cover in all seasons. This decrease is followed by the increase of LST due to the industrial area. Apart from the seasonality, the absolute maximum was observed at this district (after 4000 m). The following built-up areas show a mostly steady temperature (with some exceptions). Besides the sections crossing the rivers, the absolute minimum values were characteristic for the Liget (the biggest park in Új-Szeged district) in all seasons except for winter. The winter curve was much more balanced, and the minimum was detected in the case of the forest area near the border of the urban area. The temperature of the water surfaces (at 7000 and 9000 m) was extremely low in all cases.

Table 3 Statistical parameters of seasonal LST in the different local climate zones

| LCZ | LCZ name         | MIN         | MAX         | MEAN        | MIN         | MAX         | MEAN        | MIN         | MAX         | MEAN        | MIN         | MAX         | MEAN        |
|-----|------------------|-------------|-------------|-------------|-------------|-------------|-------------|-------------|-------------|-------------|-------------|-------------|-------------|
| 2   | Compact midrise  | 28.8        | 35.8        | <b>33.8</b> | 32.8        | 39.7        | 38.1        | 22.6        | 28.2        | 27.0        | 11.2        | 18.9        | <b>16.9</b> |
| 3   | Compact low-rise | 28.6        | 35.4        | 33.0        | 33.2        | 39.5        | 37.5        | 23.3        | 28.3        | 26.9        | 13.2        | 18.9        | <b>17.1</b> |
| 5   | Open mid-rise    | 22.1        | 38.1        | 30.2        | 28.6        | 42.1        | 36.3        | 20.8        | 30.5        | 25.7        | <b>8.0</b>  | 21.0        | 16.3        |
| 6   | Open low-rise    | 23.7        | 41.0        | 31.0        | 28.6        | 43.6        | 36.4        | 21.1        | 31.4        | 26.0        | 9.8         | 24.3        | 16.3        |
| 8   | Large low-rise   | 22.7        | <b>44.0</b> | 32.4        | 28.3        | <b>47.2</b> | <b>38.2</b> | 20.7        | <b>34.8</b> | <b>27.0</b> | 9.2         | <b>28.2</b> | 16.8        |
| 9   | Sparsely built   | <b>21.6</b> | 41.6        | <b>27.5</b> | <b>26.9</b> | 44.7        | <b>34.7</b> | <b>20.4</b> | 32.3        | <b>24.6</b> | 8.6         | 25.4        | <b>15.4</b> |
|     | Total area       | 21.9        | 34.5        | 27.7        | 26.3        | 37.5        | 32.4        | 19.3        | 27.4        | 23.3        | 10.0        | 22.8        | 16.5        |
|     |                  | 18-May-2015 |             |             | 21-Jul-2015 |             |             | 23-Sep-2015 |             |             | 22-Feb-2016 |             |             |

Table 4 Extremities in the relationship between average seasonal LST and NDVI values for district

| District  | R            | LSTmean     | NDVImean | R            | LSTmean | NDVImean    | R            | LSTmean | NDVImean |
|-----------|--------------|-------------|----------|--------------|---------|-------------|--------------|---------|----------|
| Belváros  | <b>-0.56</b> | 32.58       | 0.42     | <b>-0.59</b> | 37.14   | 0.40        | <b>-0.53</b> | 26.72   | 0.39     |
| Móráváros | <b>-0.88</b> | 29.18       | 0.60     | <b>-0.83</b> | 35.09   | 0.55        | <b>-0.81</b> | 25.44   | 0.56     |
|           |              | 18-May-2015 |          | 21-Jul-2015  |         | 21-Sep-2015 |              |         |          |



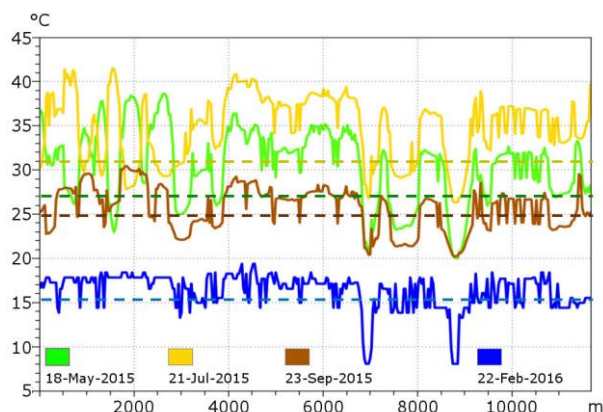


Fig. 6 Temporal patterns of LST (the dashed line represents the mean temperature of the rural areas)

The evaluation of the cross-section confirms how important the vegetation cover is in urban areas influencing the urban surface temperature. Vegetated surface can decrease the LST even by 13°C contributing to better health conditions and a positive human comfort.

## CONCLUSION

The study investigated the differences of urban surface temperature compared to rural areas. The results confirmed to what rate green areas can decrease LST which has indirect impact on the air temperature. The high density of built-up areas and the huge paved surfaces are characterized by intensive warming up. In the investigated 30-years-long period the LST pattern changed only due to the new built-up areas and other urban developments. However, the absolute numbers are highly dependent on the actual weather conditions. Compared to the rural areas the SUHI intensity has significantly decreased, which is due to the increasing extent of built-up areas. The seasonal assessment confirmed the inverse correlation between vegetation and LST.

Remote sensing and GIS assessments proved to be useful tools for mapping spatial and temporal patterns of urban surface temperature. The results can be used for city planning and management in environmental and physiological aspects as well to manage the phenomenon of UHI. The advantage of the applied GIS method is the automation of the data processing, as a result of which homogenous data can be generated for large areas. The basic datasets can be downloaded for free and the temporal extent is more than 30 years. The disadvantage is the low temporal resolution, preventing the investigating of changes within one day.

## References

- Chavez, P.S. 1996. Image-Based Atmospheric Corrections. Revisited and Improved Photogrammetric Engineering and Remote Sensing 62, 1025–1036.
- Gábor P., Jombach S. 2009. The relation between biological activity and the land surface temperature in Budapest. *Applied Ecology and Environmental Research* 7, 241–251. DOI: 10.15666/aeer/0703\_241251
- Kruse, F. A., Lefkoff, A.B., Boardman, J.B., Heidebrecht, K.B., Shapiro, A.T., Barloon, P.J., Goetz, A.F.H. 1993. The Spectral Image Processing System (SIPS) - Interactive Visualization and Analysis of Imaging spectrometer Data. *Remote Sensing of Environment* 44, 145–163. DOI: 10.1016/0034-4257(93)90013-n
- KSH 2015. Magyarország településhálózata 2. Városok-falvak. (The Hungarian settlement system 2 – Cities and villages) Central Statistical Office, Budapest, 88 p. (In Hungarian)
- Landsberg, H.E. 1981. The urban climate. The Academic Press, London, New York, 196 p.
- Lelovics E., Unger J., Gál T. 2014. Designing of an urban monitoring network, based on Local Climate Zone Mapping and temperature mapping modelling. *Climate Researches* 60, 51–62. DOI: 10.3354/cr01220
- Mallick, J., Singh, C.K., Shashtri, S., Rahman, A., Mukherjee, S. 2012. Land surface emissivity retrieval based on moisture index from LANDSAT TM satellite data over heterogeneous surfaces of Delhi city. *International Journal of Applied Earth Observation and Geoinformation* 19, 348–358. DOI: 10.1016/j.jag.2012.06.002
- Moran, M., Jackson, R., Slater, P., Teillet, P. 1992. Evaluation of simplified procedures for retrieval of land surface reflectance factors from satellite sensor output. *Remote Sensing of Environment* 41, 169–184. DOI: 10.1016/0034-4257(92)90076-v
- Nichol, J. 2005. Remote sensing of urban heat island by day and night. *Photogrammetric Engineering & Remote Sensing* 71, 613–621. DOI: 10.14358/pers.71.5.613
- OGIMET 2016. <http://www.ogimet.com/gsynres.phtml.en>
- Oke, T.R. 1976. The distinction between canopy and boundary layer urban heat islands. *Atmosphere* 14, 268–277.
- Oke, T.R. 1988. Street design and urban canopy layer climate. *Energy and Buildings* 11, 103–113. DOI: 10.1016/0378-7788(88)90026-6
- OMSZ (Hungarian Meteorological Service) 2016. <http://met.hu/eghajlat/>
- Péczely Gy. 1979. Éghajlattan (Climatology). Nemzeti Tankönyvkiadó, Budapest, 324 p. (In Hungarian)
- Probáld F. 1974. Budapest városklimája (Urban climate of Budapest). Akadémiai Kiadó, Budapest, 126 p. (In Hungarian)
- Purnhauser P. 2001. A városi hősziget és a városi szerkezet összefüggéseinek feltárása terepi és térinformatikai módszerekkel Szegeden. (Assessment of the relationship between urban heat island and city structure using field data and remote sensing). University of Szeged, Department of Climatology and Landscape Ecology, Szeged, 65 p. (In Hungarian)
- Roth, M., Oke, T.R., Emery, W.J. 1989. Satellite-derived urban heat islands from three coastal cities and the utilization of such data in urban climatology. *International Journal of Remote Sensing* 10, 1699–1720. DOI: 10.1080/01431168908904002
- Sobrino, J., Jiménez-Muñoz, J.C., Paolini, L. 2004. Land surface temperature retrieval from LANDSAT TM 5. *Remote Sensing of Environment* 90, 434–440. DOI: 10.1016/j.rse.2004.02.003
- Soósné, D.Zs. 2009. A magyarországi és közép-európai nagyvárosokban kialakuló városi hősziget vizsgálata finom felbontású műholdképek (Analysis of urban heat island effect in Hungarian and Central European cities using high-resolution satellite imagery). PhD Theses. ELTE Department of Meteorology, Budapest, 112 p. (In Hungarian)
- Stewart, I.D., Oke, T.R. 2012. Local climate zones for urban temperature studies. *Bulletin of the American Meteorological Society* 93 (12), 1879–1900. DOI: 10.1175/bams-d-11-00019.1
- Unger J. 1996. Városklimatológia – Szeged városklimája (Urban climatology – Urban climate in Szeged). Acta Climatologica et Chorologica Univ Szegediensis 31B (Urban climate special issue), 69 p. (in Hungarian)
- Unger, J. 2010a. A városi hősziget-jelenség néhány aspektusa (Some aspects of urban heat island phenomenon). Doctoral Thesis, Hungarian Academy of Sciences, Szeged, 107 p.
- Unger J., Gál T., Rakonczai J., Mucsi L., Szatmári J., Tobak Z., van Leeuwen B., Fiala K. 2010b. Modeling of the urban heat island pattern based on the relationship between surface and air temperatures. *Időjárás / Quarterly Journal of the Hungarian Meteorological Service* 114, 287–302.
- USGS Landsat 8, [https://landsat.usgs.gov/Landsat8\\_Using\\_Product.php](https://landsat.usgs.gov/Landsat8_Using_Product.php) [05.20.2016]
- Weng, Q., Lu, D., Schubring, J. 2004. Estimation of land surface temperature-vegetation abundance relationship for urban heat island studies. *Remote Sensing of Environment* 89, 467–483. DOI: 10.1016/j.rse.2003.11.005
- World Bank 2014. <http://datacatalog.worldbank.org/>